Electronic Supplementary Information

Integrating Surface Plasmon Resonance and Slow Photon Effects in Nanoporous Anodic Alumina Photonic Crystals for Photocatalysis

Siew Yee Lim[a,b,c], Cheryl Suwen Law[a,b,c], Lina Liu[a,d], Marijana Markovic[a,e], Andrew D. Abell[*b,c,f] and Abel Santos[*a,b,c]

[a]School of Chemical Engineering, The University of Adelaide, Adelaide, SA 5005, Australia
[b]Institute for Photonics and Advanced Sensing (IPAS), The University of Adelaide, 5005 Adelaide, Australia
[c]ARC Centre of Excellence for Nanoscale BioPhotonics (CNBP), The University of Adelaide, 5005 Adelaide, Australia
[d]School of Chemistry and Chemical Engineering, Ningxia University, 750021 Yinchuan, P.R. China
[e]Center of Chemistry, Institute of Chemistry, Technology and Metallurgy, University of Belgrade, 11000 Belgrade, Serbia
[f]Department of Chemistry, The University of Adelaide, Engineering North Building, 5005 Adelaide, Australia.

***E-Mails:** andrew.abell@adelaide.edu.au ; abel.santos@adelaide.edu.au

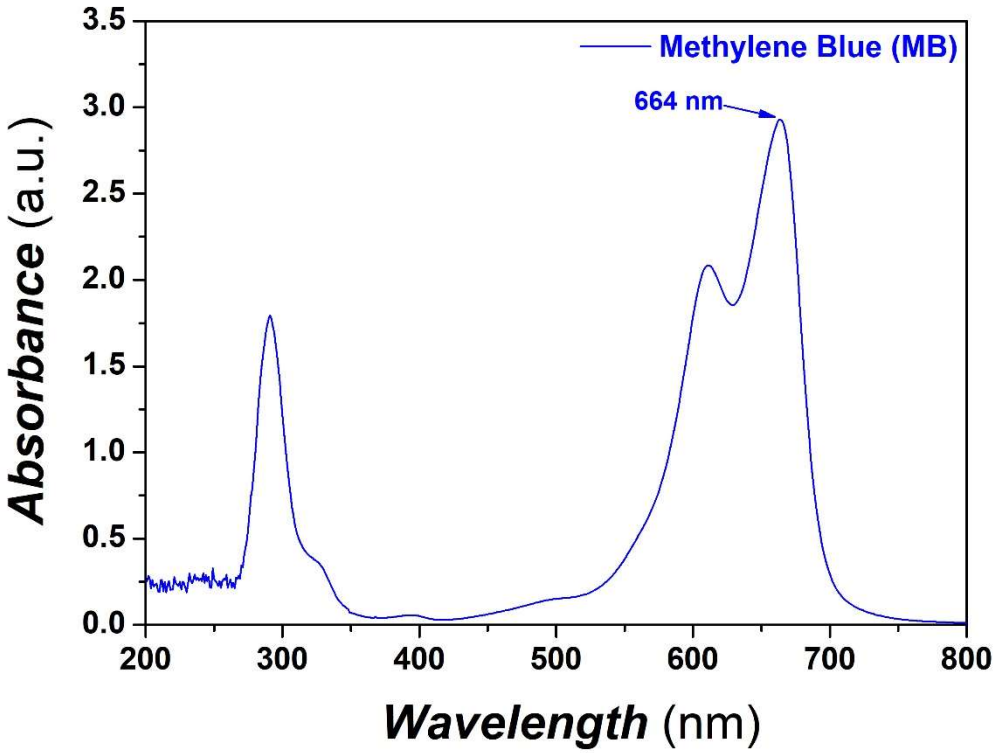

Figure S1. Absorbance spectrum of methylene blue (MB). Absorbance band maximum located at $\lambda_{abs\text{-}MB}$ = 664 nm, with an absolute absorbance intensity of ~2.9 a.u.

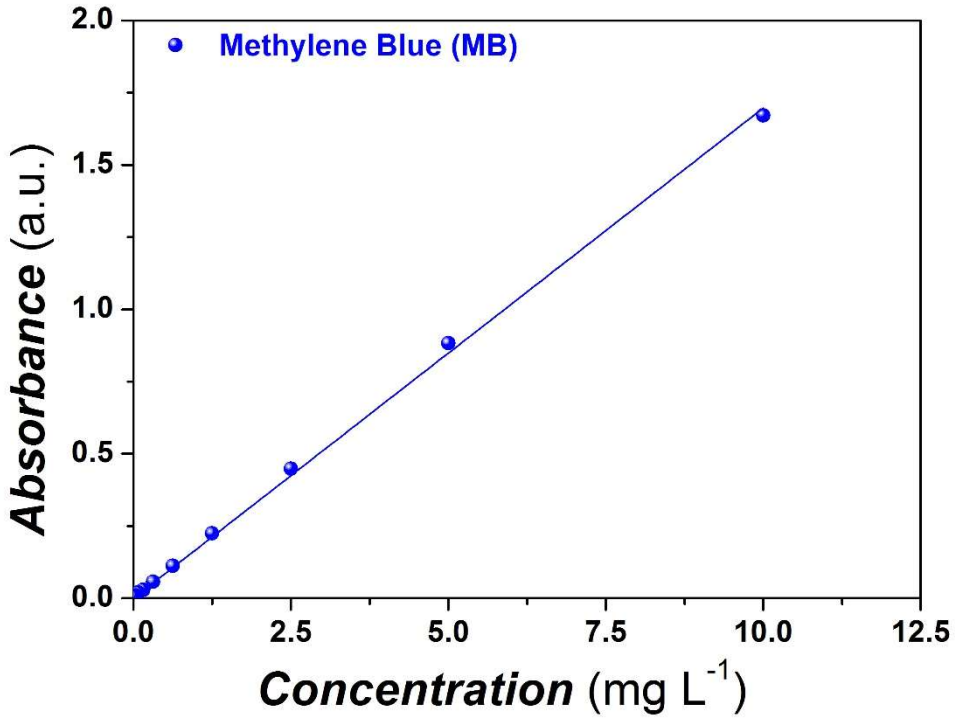

Figure S2. Linear correlation between optical absorbance and concentration of methylene blue (MB) (note: concentration range from 0.00244 to 10 mg L^{-1}). The fitting line for MB was Abs_{MB} (a.u.) = 0.1697 *[MB]* (mg L^{-1}) with R^2 = 0.99923.

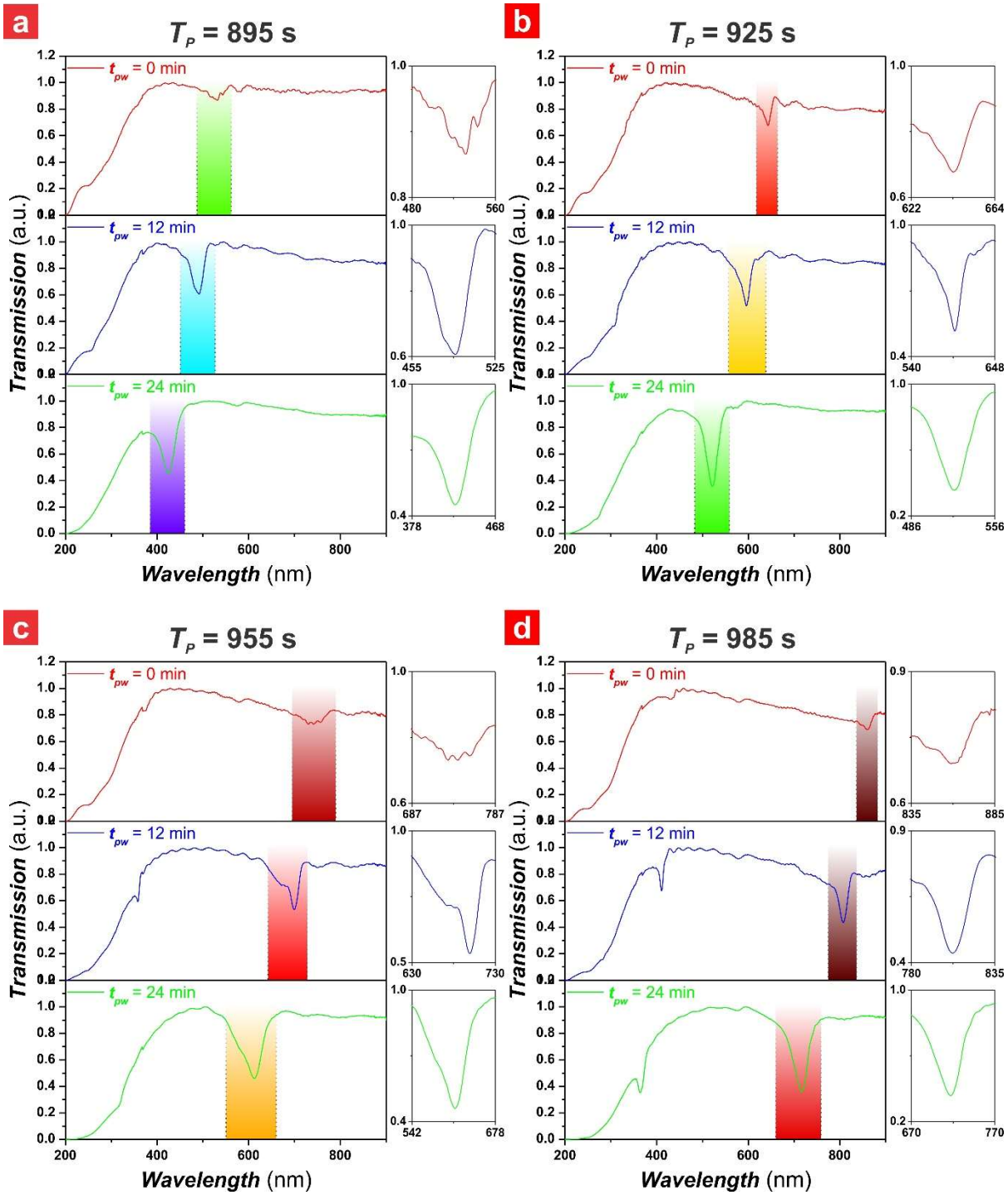

Figure S3. Transmission spectra of NAA-DBRs produced by two-step pulse anodization with anodization period (T_P) of a) 895 s, b) 925 s, c) 955 s and d) 985 s, where the medium filling the nanopores is air (note: shaded region corresponds to the magnified view of the photonic stopband displayed on the right).

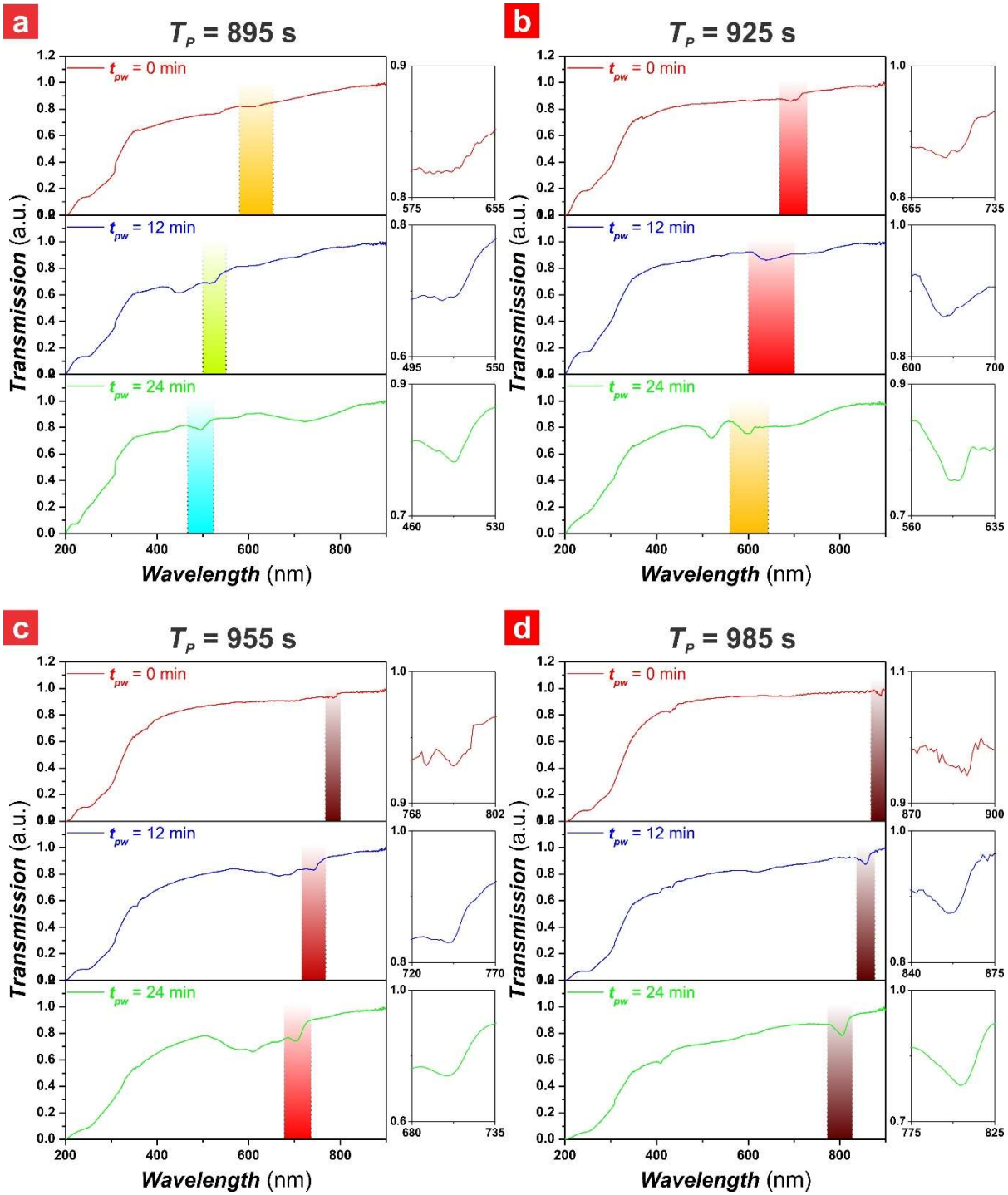

Figure S4. Transmission spectra of NAA-DBRs produced by two-step pulse anodization with anodization period (T_P) of a) 895 s, b) 925 s, c) 955 s and d) 985 s, where the medium filling the nanopores is water (note: shaded region corresponds to the magnified view of the photonic stopband displayed on the right).

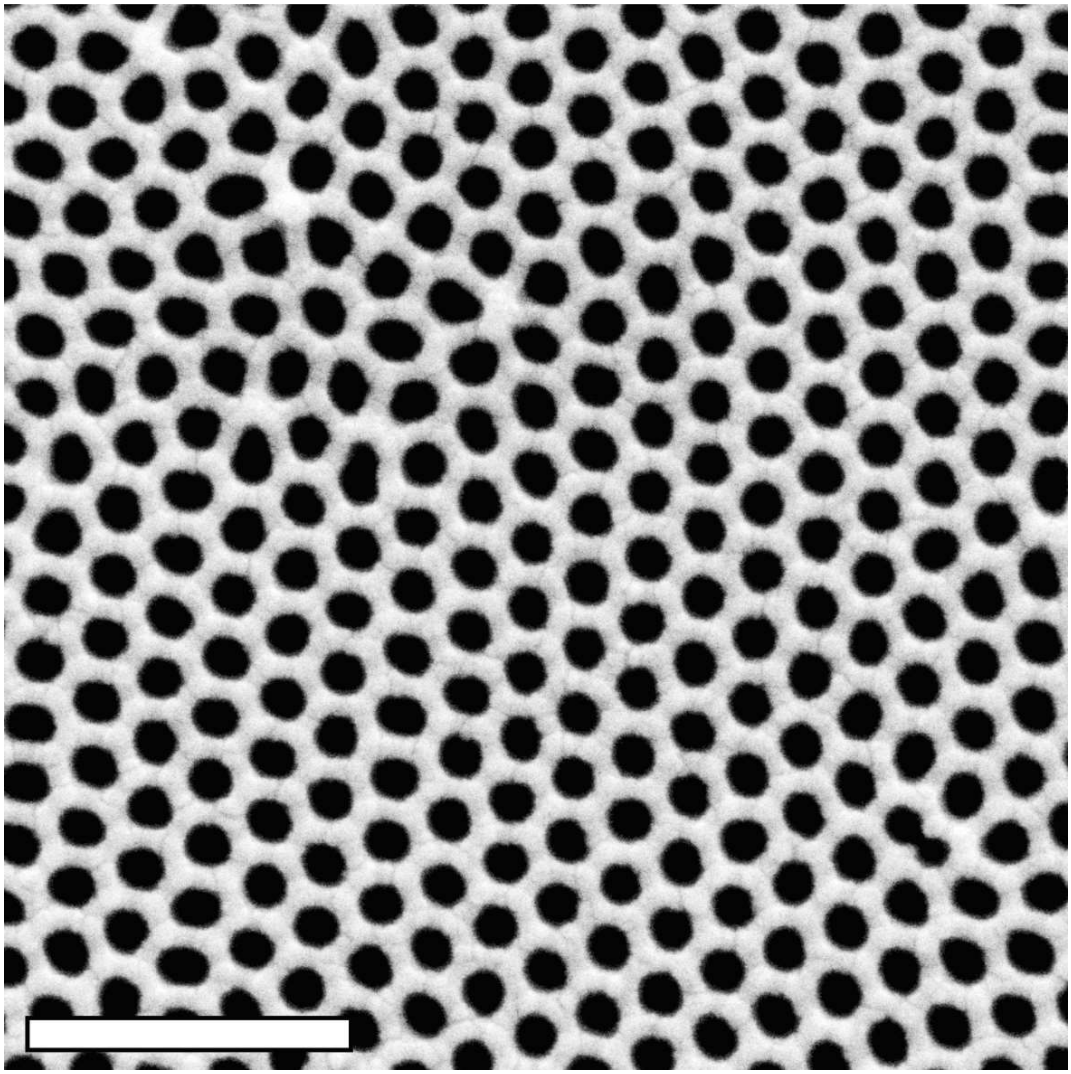

Figure S5. FEG-SEM image of a representative NAA-DBR after 30 s of Au coating (scale bar = 500 nm) (note: NAA-DBR produced with T_P = 985 s and t_{pw} = 24 min).

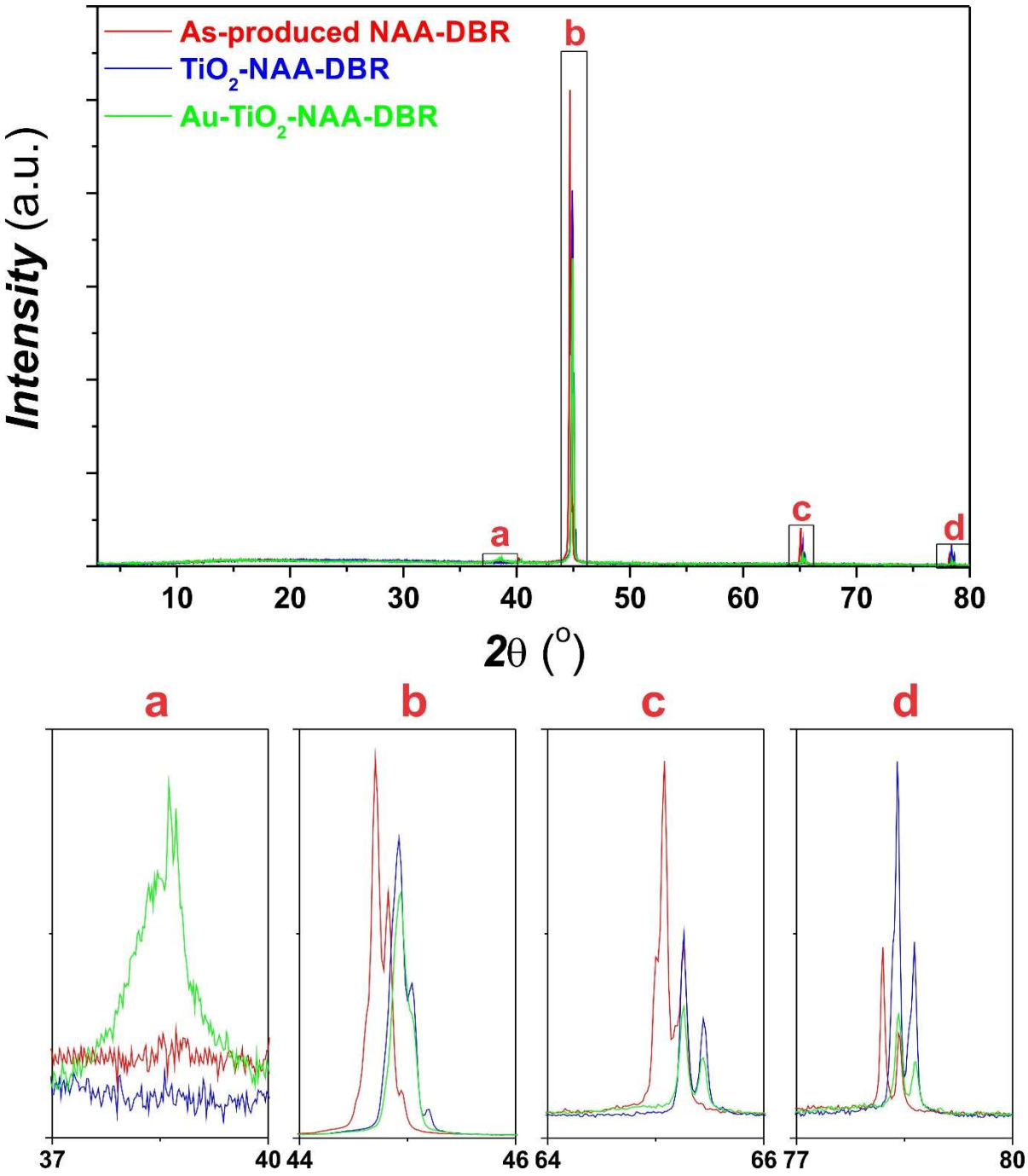

Figure S6. X-ray diffraction (XRD) spectra of a representative NAA-DBR before and after surface functionalization of TiO_2 and 30 s of Au coating (note: NAA-DBR produced with T_P = 985 s and t_{pw} = 24 min).

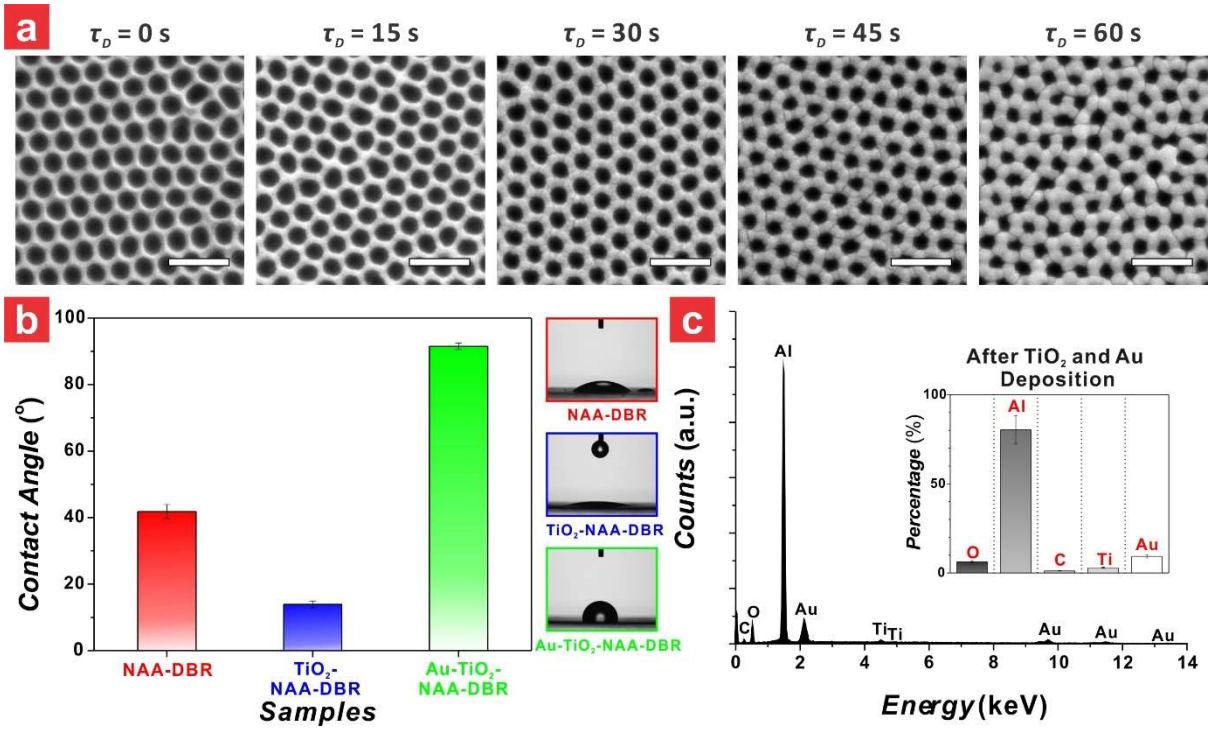

Figure S7. Structural, contact angle and chemical characterization of a representative NAA-DBR before and after surface functionalization with TiO_2 and coating with Au (note: NAA-DBR produced with T_P = 985 s and t_{pw} = 24 min). a) Top view FEG-SEM images of the NAA-DBR as a function of Au deposition time (τ_D). b) Influence of deposition of TiO_2 followed by Au coating on the contact angle (left) and digital image (right) of the as-produced NAA-DBR. c) Energy dispersive X-ray (EDX) spectrum of the representative NAA-DBR deposited with TiO_2 and 30 s Au with inset showing the percentage of main elements present in the photonic crystal structure (right).

Figure S7 - Discussion

Figure S7 provides a set of characterizations of a representative NAA-DBR produced with T_P = 985 s and t_{pw} = 24 min that demonstrate the successful deposition of TiO_2 and Au onto the inner and top surface of the nanoporous PC structure:

- FEG-SEM: Figure S7a compiles a set of top view FEG-SEM images of the TiO_2-modified NAA-DBR at different deposition time (τ_D), from τ_D = 0 to 60 s (i.e. 0, 15, 30, 45 and 60 s). Image analysis of these images reveals that the pore diameter (d_p) of the TiO_2-NAA-DBR is reduced with increasing Au deposition time, from d_p = 81 ± 6 nm at τ_D = 0 s to d_p = 50 ± 6 nm at τ_D = 60 s.
- Contact Angle: The successful functionalization of TiO_2 and deposition of Au were further validated and analyzed by contact angle measurements (Figure S7b). The contact angle for the NAA-DBR platform at different fabrication stages (i.e. as-produced, TiO_2 coating, and Au deposition) was measured by a tensiometer (Attension Theta optical tensiometer), using the sensile drop method. A water droplet was formed on the end of a syringe, which descended until the water droplet touched the surface of the NAA-DBR. After contact, the syringe was withdrawn from the surface of the NAA-DBR. Image analysis (i.e. Figure S7b – right) was used to establish the contact angle on the surface of the NAA-DBR platform before and after deposition of TiO_2 and Au (i.e. Figure S7b – left). After functionalizing the surface of the NAA-DBRs with TiO_2, the contact angle was found to decrease from 41 ± 2 to 14 ± 1^o. This indicates that TiO_2-NAA-DBRs are more hydrophilic than as-produced NAA-DBRs, and the change observed in the contact angle further demonstrates the successful functionalization of the NAA-DBR by TiO_2. A significant increase in the contact angle (i.e. 78 ± 1^o) of TiO_2-NAA-DBRs was observed after coating with the Au coating, indicating that Au-TiO_2-NAA-DBRs are significantly more hydrophobic than their TiO_2-NAA-DBR counterparts. This analysis implies that Au layers were successfully deposited onto the top surface of TiO_2-NAA-DBRs.
- Energy dispersive X-Ray Analysis (EDX): Figure S7c shows EDX spectra of a representative Au-TiO_2-NAA-DBR. The percentage of elements such as Al, Au, O, Ti and C were 80.4 ± 8.0, 9.3 ± 0.9, 6.3 ± 0.6, 2.9 ± 0.3 and 1.2 ± 0.1 %, respectively. These atoms correspond to the chemical composition of the composite photonic structure, where Al, Ti and O atoms correspond to alumina (Al_2O_3) and titania (TiO_2), C atoms correspond to contaminants incorporated into the alumina structure from the acid electrolyte (i.e. oxalic acid) during anodization, and Au atoms correspond to the Au layer deposited onto the top surface of the composite PC structure.

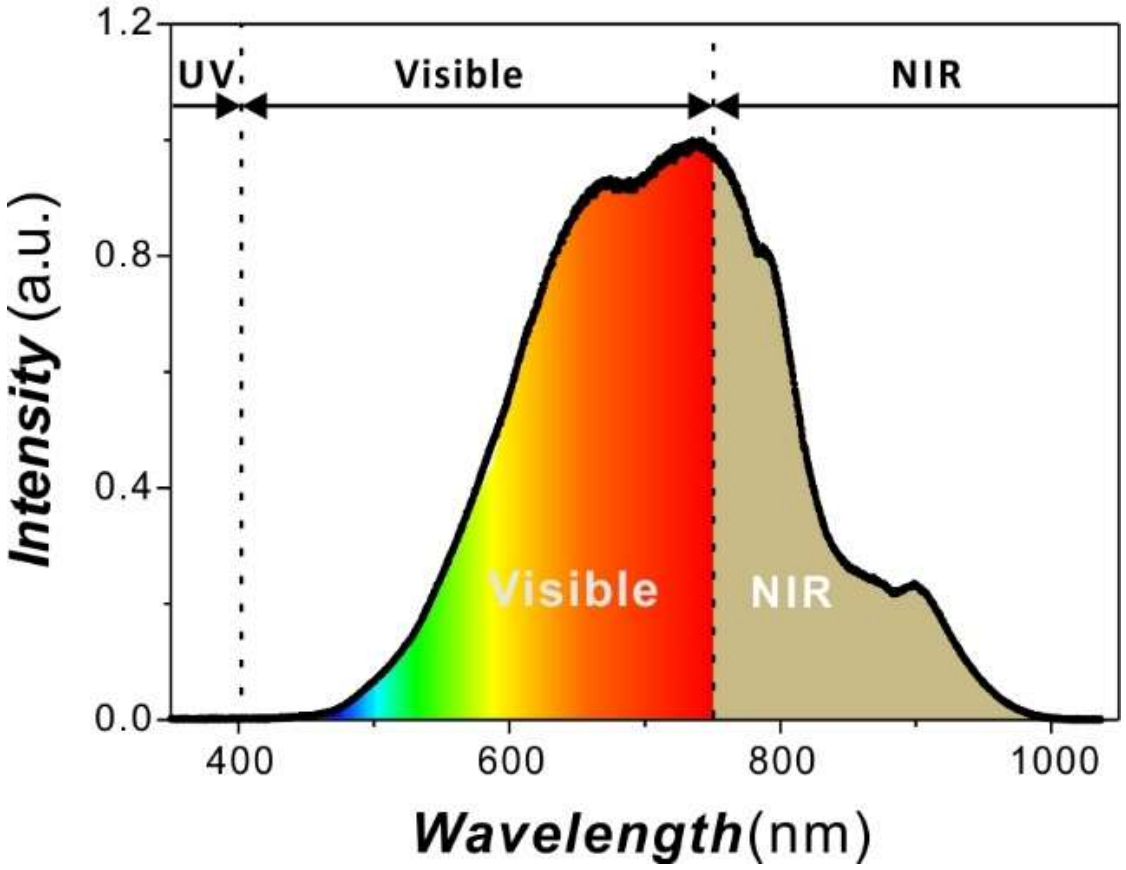

Figure S8. Spectrum of a simulated solar light irradiation source (i.e. 0.12% UV, 64.60% visible and 35.28% NIR) used for the photocatalytic degradation of methylene blue (note: the spectrum was measured using an optical fiber spectrophotometer – USB 4000, Ocean Optics, USA).

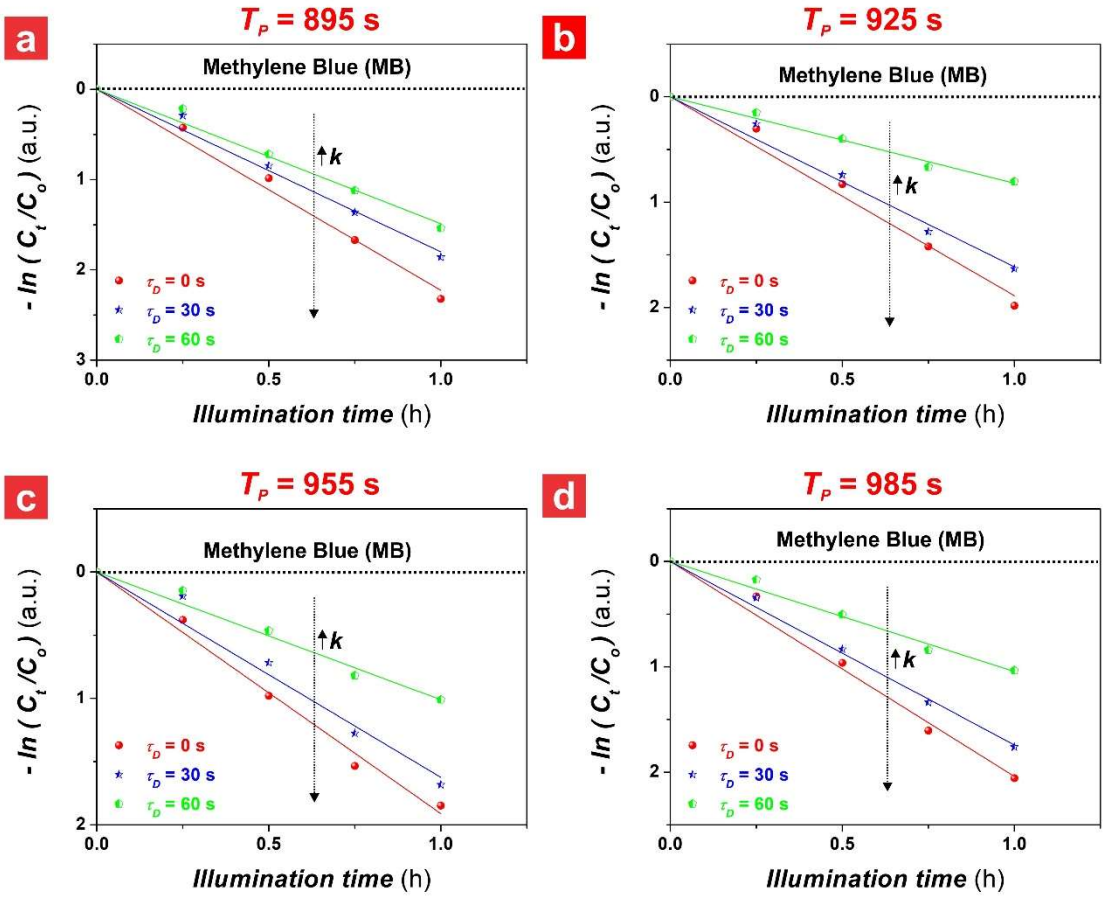

Figure S9. Photocatalytic degradation kinetics of methylene blue (MB) by Au-TiO_2-NAA-DBRs fabricated by two-step pulse anodization with t_{pw} = 12 min, Au deposition time from τ_D = 0, 30 and 60 s and anodization period T_P = a) 895 s, b) 925 s, c) 955 s and d) 985 s (note: black dotted lines correspond to the photodegradation of MB in control NAA-DBRs without the photoactive TiO_2 layer).

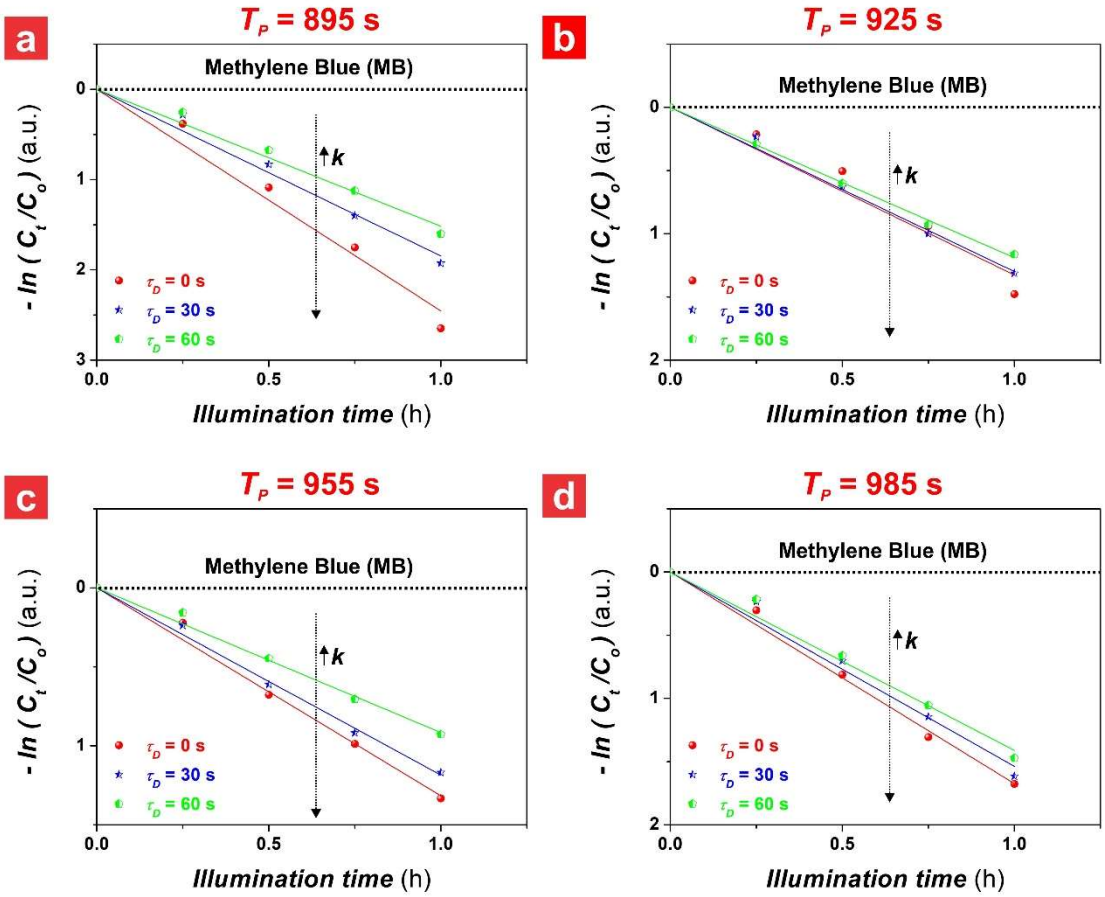

Figure S10. Photocatalytic degradation kinetics of methylene blue (MB) by Au-TiO_2-NAA-DBRs fabricated by two-step pulse anodization with t_{pw} = 24 min, Au deposition time from τ_D = 0, 30 and 60 s and anodization period T_P = a) 895 s, b) 925 s, c) 955 s and d) 985 s (note: black dotted lines correspond to the photodegradation of MB in control NAA-DBRs without the photoactive TiO_2 layer).

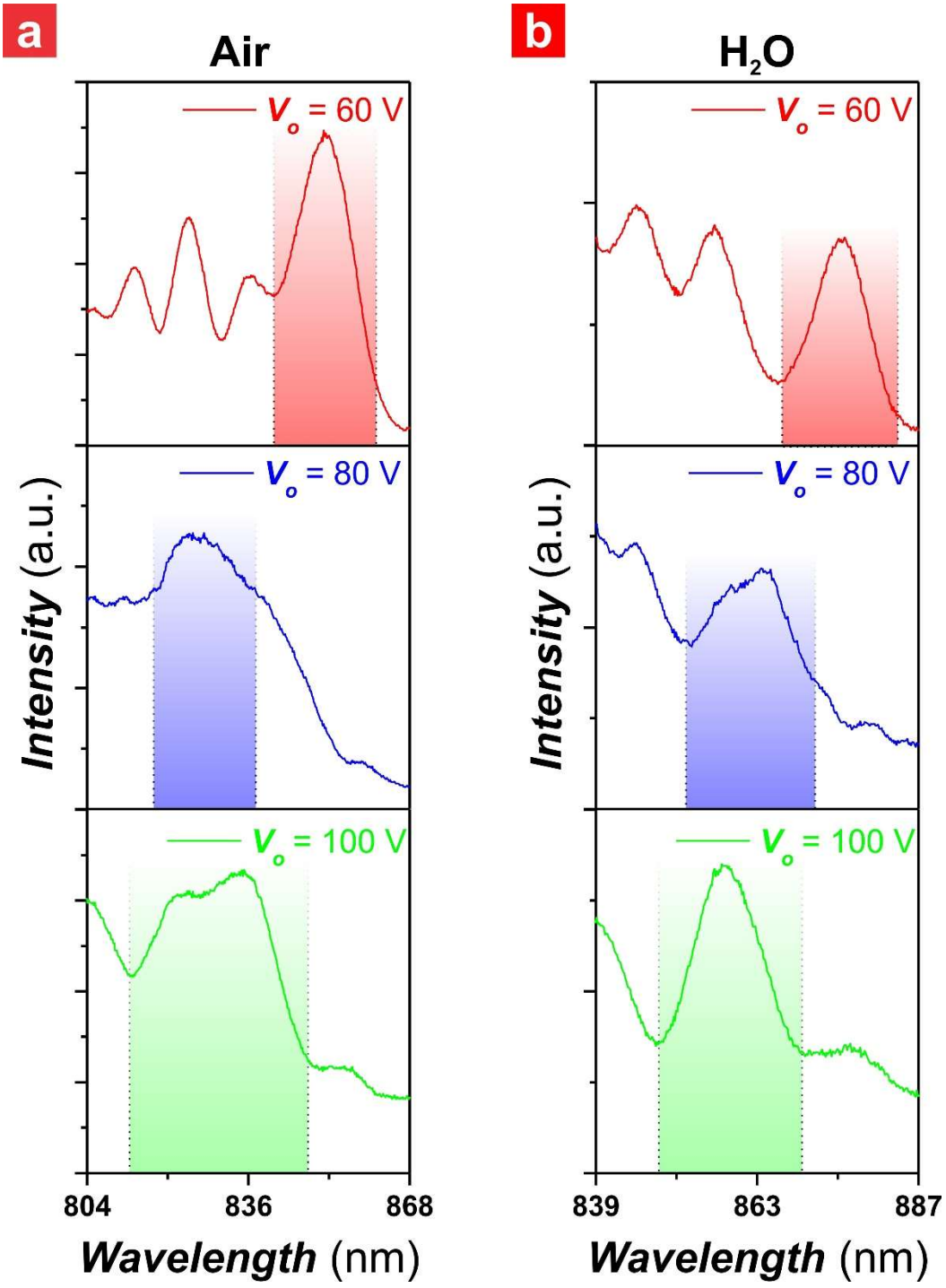

Figure S11. Reflection spectra of NAA-DBRs fabricated by three-step pulse anodization with different starting anodization voltage V_o = 60, 80 and 100 V, where the media filling the photonic structures are a) air and b) water (H_2O), respectively (note: shaded region denotes the position of the photonic stop band).

Table S1. Values of the kinetic constant (k) for the photodegradation of MB molecules by Au-TiO_2-NAA-DBRs produced by two-step pulse anodization with various pore widening time (t_{pw}), Au deposition time (τ_D) and anodization period (T_P).

t_{pw} (min)	τ_D(s)	T_P (s)	k (h^{-1})
0	0	895	1.83 ± 0.06
		925	1.26 ± 0.04
		955	2.22 ± 0.08
		985	1.57 ± 0.05
	30	895	1.46 ± 0.04
		925	1.13 ± 0.04
		955	1.98 ± 0.07
		985	1.32 ± 0.06
	60	895	1.02 ± 0.06
		925	0.76 ± 0.02
		955	1.35 ± 0.05
		985	0.93 ± 0.04
12	0	895	2.23 ± 0.08
		925	1.89 ± 0.08
		955	1.91 ± 0.06
		985	2.04 ± 0.07
	30	895	1.80 ± 0.07
		925	1.61 ± 0.06
		955	1.62 ± 0.09
		985	1.74 ± 0.04
	60	895	1.49 ± 0.06
		925	0.82 ± 0.03
		955	1.01 ± 0.05
		985	1.04 ± 0.04
24	0	895	2.45 ± 0.13
		925	1.33 ± 0.09
		955	1.32 ± 0.04
		985	1.67 ± 0.05
	30	895	1.85 ± 0.08
		925	1.30 ± 0.04
		955	1.19 ± 0.03
		985	1.54 ± 0.07
	60	895	1.52 ± 0.06
		925	1.19 ± 0.02
		955	0.92 ± 0.03
		985	1.41 ± 0.06

Table S2. Values of the kinetic constant (k) for the photodegradation of MB molecules by TiO_2-NAA-DBRs produced with T_P = 985 s and t_{pw} = 24 min, and different top coatings (i.e. Au and Ag) and deposition time (τ_D).

Top Coating	τ_D (s)	k (h^{-1})
Au	0	1.67 ± 0.05
	30	1.54 ± 0.07
	60	1.41 ± 0.06
Ag	0	1.67 ± 0.05
	30	1.44 ± 0.06
	60	1.35 ± 0.05

Table S3. Values of the kinetic constant (k) for the photodegradation of MB molecules by Au-TiO_2-NAA-DBRs produced by three-step pulse anodization with different starting anodization voltage (V_o) and Au deposition time (τ_D).

V_o (V)	τ_D (s)	k (h^{-1})
60	0	1.26 ± 0.03
	30	1.25 ± 0.07
	60	1.02 ± 0.03
80	0	1.52 ± 0.07
	30	1.10 ± 0.03
	60	0.61 ± 0.03
100	0	1.51 ± 0.05
	30	1.02 ± 0.06
	60	0.59 ± 0.06